HIGH-RESOLUTION AIRBORNE LIDAR/CCD MAPPING OF SAN ANDREAS FAULT

Charles Toth, Dorota A. Grejner-Brzezinska and Michael Bevis
The Center for Mapping
Satellite Positioning and Inertial Navigation (SPIN) Laboratory
The Ohio State University
E-mail: toth@cfm.ohio-state.edu

Abstract: To support earthquake research, a dedicated LiDAR (Light Detection and Ranging) survey was conducted to map an approximately 1,000 km segment of the San Andreas Fault in southern California in the spring of 2005. The Ohio State University-led team included NCALM (National Center for Airborne Laser Mapping) from the University of Florida, USGS (United States Geological Survey), UNAVCO and Optech International. The project was funded by the National Science Foundation, and the primary objective was to create a highly accurate DEM (Digital Elevation Model) along the fault line before the Big One happens. To achieve the highest possible accuracy, extreme care was devoted to all the system components and the mission planning of the LiDAR survey. A dense network of GPS reference stations was established in addition to the PBO (Plate Boundary Observation) system to provide short baselines for the sensor platform orientation. The Optech 3100 ALTM system was operated at a 70 kHz pulse rate, which provided an optimum in terms of ranging accuracy, area coverage and point density. For QA/QC (quality assurance/quality control) as well as for possible corrections, conventional profiles were surveyed, and LiDAR-specific targets were used. These targets provided not only the vertical correction, but were also able to improve the horizontal accuracy (relative to the laser pulse footprint size). This paper provides a short project overview and a preliminary analysis of the achieved accuracy.

1. Introduction

Project B4 is an NSF project led by the OSU and USGS scientists, and supported by NCALM and UNAVCO (a non-profit, membership-governed consortium, supporting Earth science). The team completed an Airborne Laser Swath Mapping (ALSM) survey of ~ 1,000 km of the southern San Andreas Fault and San Jacinto Fault systems in mid-2005. The main purposes of this project are (1) to capture in great detail the geometry of the near-field of these faults prior to the Big One, so that after a great earthquake occurs the survey can be repeated to examine the near-field displacements (coseismic and postseismic) in extraordinary detail, and thereby resolve some of the great debates about earthquake source physics, (2) provide our present results to geomorphologists and paleoseismologists, who can use offsets in topography to address the history of major earthquakes along these faults, and to guide the selection of new trenching sites and dating (3) improve the near-field geodetic infrastructure of these fault systems. Large numbers of volunteers played a crucial role in the original field measurements, and we hope the project team will continue to grow as we move from raw data, through preliminary data products, to the refined and higher level data products.

2. Project Area

The project is aimed to investigate the primary continental transform fault of the North American – Pacific plate boundary, the southern San Andreas fault (SSAF), see Figure 1, from just northwest of Parkfield to Bombay Beach, California (e.g., [10], [11] and [7]). This section of the fault includes the transition from creeping to locked zones along-strike at the northwestern end, as well as what is known as the Big Bend and both tectonic 'knots' at Tejon Pass and San Gorgonio Pass (e.g., [9]). Furthermore, it includes perhaps the most heavily primed section of the entire San Andreas fault that runs down the Coachella Valley to its southeastern terminus at Durmid Hill. Of the many possible "Big Ones" on the southern San Andreas fault, the acquired dataset is likely to cover them all. If the pre-event imagery obtained by this study were to be differenced with post-event imagery, an unprecedented mapping of the near-fault pattern of deformation would result in a very high-resolution three-dimensional displacement field along the entire rupture zone.
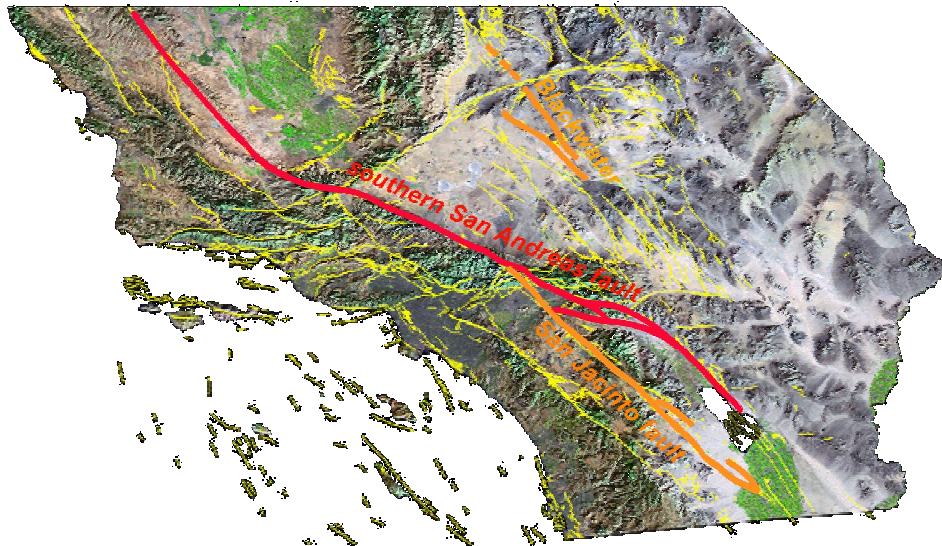

Figure 1: The southern San Andreas and San Jacinto faults.

From Cajon Pass towards the southeast to Whitewater is a section that remains highly controversial, since some investigators believe it has accumulated as much as 14 meters of slip since the last event, whereas others feel that it may have slipped as recently as 1812 or 1857 and hence has little accumulated strain (e.g., [8]). The San Bernardino Mountains to the north, and San Jacinto Mountains to the south, press together across the multiple traces of the San Andreas fault zone. Some 10-15 mm/yr of right-lateral shear strain makes its way around the east end of the Big Bend, from the San Andreas fault in the Coachella Valley (near Indio and Palm Springs) to the Eastern California Shear Zone (ECSZ; near Yucca Valley and Landers). A similar amount may feed from the San Jacinto fault to the Mojave segment of the San Andreas fault (to the northwest from Cajon Pass). The amount of strain occurring within this complex portion is not clear, but may be as little as 5 mm/yr or as much as 15 mm/yr. Recent studies of the Coachella Valley segment confirm that several hundred years have elapsed while the fault continues to accumulate strain at a high rate (e.g., [4]), clearly indicative of a strong proclivity towards future seismic rupture.

3. Data Acquisition Campaign

The airborne surveys took place May 15-25. 2005. A Cessna 310 aircraft was hired and Optech International provided the ALTM 3100 system at no cost to the project. NCALM was in the charge of the flight operations. OSU was the lead team for the GPS work that was assisted by UNAVCO and USGS Pasadena staff. The ground LiDAR target and profiling operations were supported by two OSU teams.

The airborne sensor suite included:

- The state-of-the-art Optech 3100 system configured for 70 kHz pulse rate. This represented an optimal balance between the high spatial resolution of the LiDAR points and a good accuracy for the range measurements.

- An experimental color-infrared digital camera was installed next to the Optech 3100 system, providing 1K by 2K resolution imagery in four bands; images were acquired synchronized to the 1PPS GPS signal (1 FPS).

- In addition to the built-in Applanix POS component of the Optech 3100 system, a Honeywell H764G IMU unit were installed in the airplane. The increased redundancy offered a potential for improved QA/QC processes as well as for better combined georeferencing results.

The project area encompassing about 1,000 km fault lines was segmented in 15 sections, including the San Andreas and San Jacinto fault lines (SAF and SJF). Each segment was about 50 km long and to achieve an about 1,000 m swath with double coverage, 5-6 flights were flown. On a typical day, two segments were mapped, each requiring about a net 2 hours of sensor-on time.

To achieve the highest possible georeferencing performance of the airborne platform, a dense network of GPS base stations was established along the fault line. About 100 new stations were set up at an average spacing of 10 km. The stations were occupied for 6-10 hours to support the LiDAR flights, as well as to allow for reference them to the POB system; the POB reference stations were switched to 1 Hz data acquisition rate for the duration of the data acquisition campaign.

For QA/QC of the surface points, as well as for the additional LiDAR strip corrections, mobile LiDAR-specific targets were used throughout the surveys. Typically, two clusters of 3-4 targets were placed along the about 50 km flight segments. The target cluster were location was planned for around 1/3 and 2/3 of the segment length. However, due to access difficulties, such as excessive drive time or lack of drivable roads, the actual location varied on a wider scale.

The total number of personnel involved in the airborne and ground surveys was about 30, including project leaders from OSU and USGS, staff from NCALM and UNAVCO, students and volunteers.

4. Data Processing

The 10-day of intense airborne and ground surveys produced a massive amount of data, presenting a rather complex and time-consuming processing task for the team. First the GPS reference station network was processed, and then, based on that results the flight lines were processed to create the initial LiDAR point datasets to meet the delivery of a preliminary product, expected by the earthquake research community. In the second phase, refinements

are applied in every stage of the processing to achieve the highest possible accuracy of the end products. This process is still going on and final results are expected later this year. In the following, a few samples are shown to indicate selected aspects of the data processing.

4.1. Reference Station Data Processing

The GPS reference station network adjustment was performed at OSU. The GAMIT software was used for this processing task. Initial results were made available in July and the final results were released in October, 2005. The accuracy of the second adjustment reached sub-cm level, see [1].

4.2. Flight Line Processing

The flight lines were initially processed by the KARS software [6] and the results were used to merge with the Applanix IMU data to provide the sensor orientation for the LiDAR system. To achieve high reliability of the results, two independent groups performed a thorough analysis of the select flight line solutions with respect to the base stations used. Figure shows RMS_Z values for L1 and L3 (iono-free) solutions with respect to GPS reference point GC060 in segment SAF10. The true 3D difference between the trajectories was considered in the comparative studies. Results have shown that up to 20-30 km long baselines, the difference is insignificant in most cases. Once this investigation is completed, the flight lines will be reprocessed accordingly. At that stage, additional H764G IMU data will be processed by the AIMS™ suite (e.g., [5]) and comparisons will be done with the standard GPS/IMU solution.
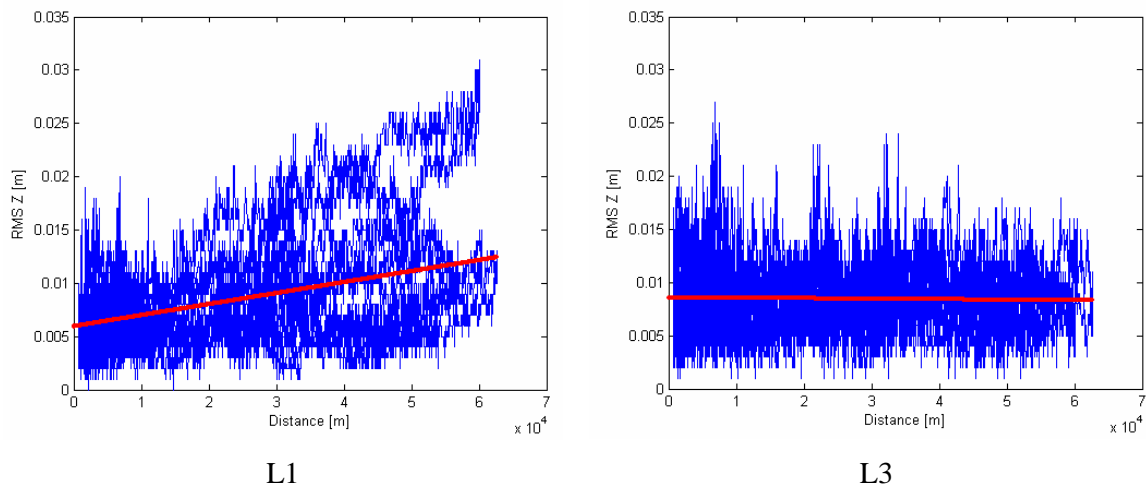

L1   L3
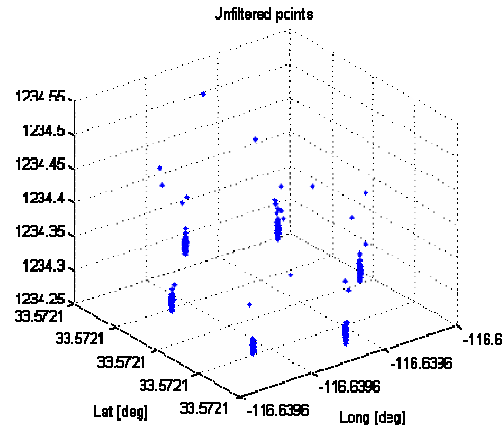
Figure 2: RMS of Z coordinates of L1 and L3 solutions.

4.3. Processing of LiDAR-specific Targets

The sensor georeferencing received an unusual attention in the B4 project, as discussed above. But even under this extreme care, ground control is the only way to validate the performance of the LiDAR product. Most of the surveyed SAF and SJF lines are in mountainous and desert areas, where there are practically no adequate objects for QA/QC. There are no paved areas or buildings, and the typical coverage is vegetation, ranging from desert shrubs to wooded landscapes. Therefore, LiDAR-specific targets and conventional profiles (transects) were used for ground control, see Figure 3a. A detailed discussion on

target design and achievable accuracy can be found in [2] and [3]. During the 10-day airborne surveying campaign, LiDAR targets were placed at an average spacing of 15 km along the 1,000 km fault line. The periphery of targets was surveyed GPS-surveyed at six positions; 5-8 minute occupation time for each location. Using the closest GPS reference station, the clusters were computed by KARS; Figure 3b shows the typical results. In subsequent processing steps, outliers were removed and the six locations were computed followed by the derivation of the center location coordinates of the target and the orientation of the target plane. Extended analysis confirmed that the typical accuracy of the target center point is 2-3 cm horizontally and 2 cm vertically.

L1   L3

Figure 3: The southern San Andreas and San Jacinto faults.

4.4. Performance Evaluation

The availability of the LiDAR-specific target data allowed for the initial assessment of the LiDAR point quality. Figure 4 shows a cluster if three targets in segment SAF1, using intensity representation.
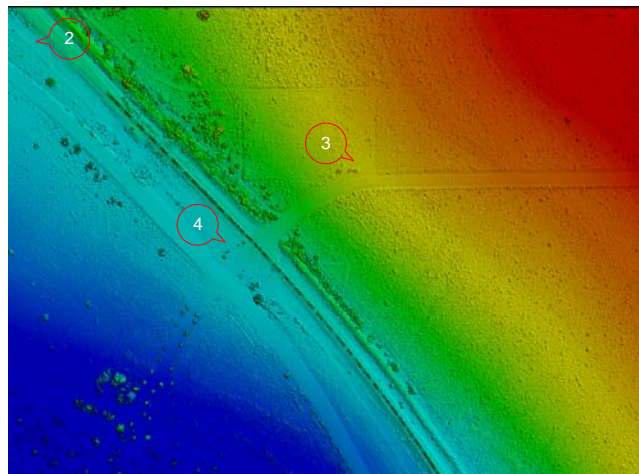

Figure 4: A cluster of three LiDAR targets.

A dedicated software utility was developed to automate the extraction of the LiDAR targets from the raw LiDAR point cloud. The output of the process is the estimated location of the centerpoint of the targets. Table below shows the results for the case shown in Figure 4, confirming a good accuracy achieved in the initial processing.

	LiDAR (NCALM) [m]			GPS-measured target [m]			Differences		
	X	Y	Z	X	Y	Z			
2	600381.57	3708592.44	-92.18	600381.55	3708592.56	-92.23	0.02	-0.12	0.05
3	600712.71	3708469.62	-82.54	600712.44	3708469.71	-82.53	0.27	-0.09	-0.01
4	600579.61	3708382.45	-92.19	600579.70	3708382.60	-92.23	-0.08	-0.15	0.04
					Average		0.07	-0.12	0.03
					STDEV		0.18	0.03	0.03

5. Conclusion

The project to map the southern San Andreas fault at unprecedented accuracy has produced encouraging initial results. Sample data indicate that the vertical LiDAR point accuracy falls in the sub-decimeter range and can be further improved where ground control is available.

References:
[1]   Bevis, M. *et.al.:* The B4 Project: Scanning the San Andreas and San Jacinto Fault Zones, *Eos Trans. AGU, 86*(52), Fall Meet. Suppl., H34B-01, 2005.
[2]   Csanyi, N, Toth, C. Grejner-Brzezinska, D. and Ray, J.: Improving LiDAR data accuracy using LiDAR-specific ground targets, ASPRS Annual Conference, Baltimore, MD, March 7-11, CD-ROM, 2005.
[3]   Csanyi, N. and Toth, C.: Improvement of LiDAR Data Accuracy Using LiDAR-Specific Ground Targets, *Photogrammetric Engineering & Remote Sensing*, (in press), 2006.
[4]   Fumal, T.E., Pezzopane, S.K., Weldon, R.J., II, and Schwartz, D.P.: A 100-year average recurrence interval for the San Andreas fault at Wrightwood, California: *Science*, v. 259, p. 199-203, 1993.
[5]   Grejner-Brzezinska D. A.: Direct Exterior Orientation of Airborne Imagery with GPS/INS System: Performance Analysis, *Navigation*, Vol. 46, No. 4, pp. 261-270, 1999.
[6]   Mader, G.L.: "Rapid Static and Kinematic Global Positioning System Solutions Using the Ambiguity Function Technique", *Journal of Geophysical Research, 97, 3271-3283,* 1992.
[7]   Matti, J.C., and Morton, D.M., Paleogeographic evolution of the San Andreas fault in southern California: a reconstruction based on a new cross-fault correlation, *in* Powell, R.E., Weldon, R.J., and Matti, J.C., eds., The San Andreas fault system: displacement, palinspastic reconstruction, and geologic evolution: *Geological Society of America Memoir 178*, p. 107-159, 1993.
[8]   McGill, S. F., and C. M. Rubin, Surficial slip distribution on the central Emerson fault during the June 28, 1992, Landers earthquake, California, *J. Geophys. Res.*, vol. 104, #B3, pp. 4811-4833, 1999.
[9]   Sykes, L.R., and Seeber, Leonardo, Great earthquakes and great asperities, San Andreas fault, southern California: *Geology*, v. 13, no. 12, p. 835-838, 1985.
[10] Wallace, R.E., ed., The San Andreas Fault system, California: *U.S. Geological Survey Professional Paper 1515*, 283 p., 1990.
[11] Wallace, R.E., Structure of a portion of the San Andreas rift in southern California: *Geological Society of America Bulletin*, v. 60, no. 4, p. 781-806, 1949.